

Thesis/
Reports
Mitic
c.m.

Structural Analysis and Flux
Associations of CO₂, H₂O, Heat and Ozone
using CODE Cotton and Grape Data

Structural Analysis and Flux Associations of CO₂, H₂O, Heat and Ozone using CODE Cotton and Grape Data

Final Report
June 12, 1997

Constance M. Mitic
Dept. Natural Resource Sciences, McGill University
Montreal, Canada, H9X-3V9
e-mail: Mitic@nrs.mcgill.ca
Tel: 514 398-7929
Fax: 514 398-7990

RM Coop. Agreement 28-C5-877

Structural Analysis and Flux Associations of CO₂, H₂O, Heat and Ozone using CODE Cotton and Grape Tower Data

Constance M. Mitic¹, William J. Massman², Peter H. Schuepp¹, Jeffery L. Collett, Jr.³

¹*Dept. Natural Resources Sciences, McGill University, Montreal, Canada;* ²*U.S. Dept. of Agriculture/Forest Service, Ft. Collins, Co.;* ³*Dept. of Atmospheric Sciences, Colorado State University, Ft. Collins, Co.*

1. INTRODUCTION

Over the past several decades much research in the atmospheric and environmental sciences has been focused on surface-atmosphere dynamics and how they may be related to changes in climate (D'Arrigo et al., 1987; Mooney et al., 1991; Field et al., 1992; Harris and Frolking, 1992; Viau and Mitic, 1992; Melillo et al., 1993; Chapman and Thurlow, 1996). The use of large scale models for climate and or weather forecasting as well as ecosystem response, has to incorporate some form of parameterization of the surface characteristics (McGuire et al., 1991; Koster and Suarez, 1992, Sellers et al., 1992; Melillo et al., 1993; Bonan, 1993; Massman et al., 1994; Goetz and Prince, 1996, Ruimy et al., 1996). The fact that these models are sensitive to variability at the surface (Wollenweber, 1995; Klaassen and Claussen, 1995; Sud et al 1988), and the uncertainty surrounding the relative of the influence of the various scales of these surface variability (Moore et al., 1993), highlights the need to improve our understanding of the atmosphere-ecosystem exchange processes. This need is reflected in the increasingly large number of studies that focus on the parameterization of surface characteristics (Hanen et al., 1995; Hall et al., 1995; Lee et al., 1996) and in particular how various fluxes are coupled to the surface (Schuepp et al., 1987; Mack et al., 1990; Hollinger et al., 1994; Massman

et al., 1993; Rochette et al., 1994; Baldocchi, 1994; Guo et al., 1995a) as well as to each other (Mitic et al., 1997).

This study uses a method developed by Mitic et al., (1997) to objectively separate the larger mesoscale flux from the local flux in order to identify the categories of scales affecting surface-atmosphere exchange process, while at the same time achieving a physically meaningful definition of the means used in the calculation of the flux estimates. Focus is placed on surface-atmosphere exchange processes at the "patch" scale (1 km^2), derived from meteorological tower observations. The objective is to characterize the temporal evolution and characteristics of coherent structures during unstable (day) and stable (night) conditions, over two different crop canopies. Due to the importance of ozone deposition in the study area and the primary objective of CODE (Pederson et al., 1995), focus is placed on the associations of ozone to the other flux variables.

Regional models such as those used for ozone deposition (Massman et al., 1994), derive estimates based on a variety of surface characteristics at different scales. However, some parameters, such as vapour and CO_2 flux, are more readily estimated than others, such as ozone flux. The general objective of this study is to increase our understanding of the association among the various fluxes and how they are tied to the characteristics of the underlying surface, to help assess the potential of estimating fluxes from surface characteristics.

Only a few studies have specifically related the distinct, coherent motions of turbulence (as opposed to incoherent noise) in the surface layer to surface characteristics (Caramori et al., 1994; Mitic et al., 1995; Mitic et al., 1997). These coherent "structures"

are responsible for the bulk of turbulent transport in the surface layer and have been examined from various other perspectives (Wyngaard, 1983; Eloranta and Forrest, 1992; Mahrt and Ek, 1993a & 1993b, Paw U et al., 1995). A study of coherent turbulent structures allows for the improvement of our understanding of the processes operating on surface fluxes. It lends insight into the degree to which various fluxes are associated with each other and with the underlying surface. Identifying the physical extent of structures and their composition, will give some indication of the driving forces operating on flux transport as well as their partitioning between the surface and the atmosphere. In this study, tower data collected at the cotton and grape sites during the California Ozone Deposition Experiment (CODE) in the summer of 1991, are used to examine flux associations of CO_2 , H_2O , heat and ozone. This is done for the two gradient modes of transport, where the surface acts as a sink for CO_2 and ozone, and a source of moisture and heat during the day, and a source of CO_2 , and a sink for heat at night.

1.1. Site and Data Description

The data used in this study were collected at two meteorological tower sites over a cotton and grape canopy during CODE, as part of the San Joaquin Valley Air Quality Study. The sites were located in the central valley of southern California at approximately 100 m above sea level. The field observation period lasted from early July to early August. Five days were selected for study from each of the two data sets. For each of these days, two 20 min time segments were used for the analyses, one during stable night time conditions and the other during unstable daytime conditions. The daytime

segments were selected from periods between midday to mid-afternoon when the boundary layer is considered to be fully developed and z/L is significantly negative. The nighttime segments have zero solar radiation and a positive z/L . The selection of the days for which the analyses is performed depended on the data quality as well as similarity in conditions such as mean wind speed and atmospheric stability conditions. Both the grape and cotton data sets include eddy correlation observations of the vertical wind component, CO_2 , H_2O , air temperature and ozone.

1.1.1. Cotton site

The tower at the cotton site was operated by the ASTER group from the U.S. National Centre for Atmospheric Research (NCAR), Boulder, Co. The site was located at $36^{\circ} 48' 50''$ N and $120^{\circ} 40' 38''$ W, 80 km west of Fresno. The crop was planted in an E-W row orientation spaced 1 m apart. During the observation period, the average height of the cotton crop increased from 0.4 m to 0.9 m, and the leaf area index increased from 1.8 to 2.5. Eddy correlation systems were located at 5 m above the surface to sample the three wind components, water vapour, CO_2 and air temperature at a frequency of 20 Hz. Data were collected continuously from July 11 to August 7, 1991. The selected days and time segments used in this study are listed in Table 1. For the selected nighttime segments, the mean wind speed ranged from 1.7 m s^{-1} to 2.2 m s^{-1} , z/L between 0.11 and 0.65, the mean surface temperature between 22°C and 24.5°C , and dew was present in all cases. The daytime segments are characterized by mean wind speeds between 1.2 m s^{-1} and 2.3 m s^{-1} , z/L between -0.19 and -2.0, mean surface temperature between 30

$^{\circ}\text{C}$ and $38.8\text{ }^{\circ}\text{C}$ and half hourly averaged incident solar radiation between 946 W m^2 and 987 W m^2 with the exception of one day (Aug. 5) where it was 750 W m^2 . The cotton fields were irrigated.

1.1.2. *Grape site*

The tower at the grape site was operated by the Air Quality Processes Research Division of the Atmospheric Environment Service, Canada. The site was located 40 km northwest of Fresno, California, at $36^{\circ} 51' 36''\text{ N}$ and $120^{\circ} 6' 7''\text{ W}$. The grape crop was planted in rows oriented in an E-W direction spaced 3 m apart. The grass growing between the rows was mowed about a week prior to the start of field measurements and grew to about 30 cm at the end of the study. The average height of the vines was 1.7 m, and the LAI remained unchanged at 3.4 for the duration of the experimental period. Data were collected continuously at the site from July 11 to August 08, 1991, at a height of 9.4 m. above the surface and at a frequency of 20 Hz. Table 1 shows the days and time segments of data used in this study. The night-time series are characterized by mean wind speeds between 1.68 m s^{-1} and 2.46 m s^{-1} , z/L between 0.22 and 1.0 and mean surface temperatures from $15.6\text{ }^{\circ}\text{C}$ to $20.7\text{ }^{\circ}\text{C}$. During the day-time segments, the mean wind speed ranged from 1.05 m s^{-1} to 3.76 m s^{-1} , z/L from -0.19 to -3.07, mean surface temperature from $28.9\text{ }^{\circ}\text{C}$ to $37.6\text{ }^{\circ}\text{C}$, and mean incident solar radiation from 837 W m^2 to 967 W m^2 . The grape site was irrigated twice during the observation period.

Details of the instrumentation and site characteristics for both sites may be found in Massman et al., (1994).

2. DATA ANALYSIS

The analytical procedures used to define the flux estimates for CO₂, H₂O, heat and ozone, identify the coherent structures and examine the relationships and associations between the various flux components transported by these structures are similar to those used by Mitic et al. (1997) on aircraft data, where a more detailed explanation may be found. However, while Mitic et al. (1997) provided a spatial analysis of flux and the corresponding coherent structures, this paper is concerned with their temporal distribution and characteristics at the stationary observation point. The mean used to estimate the flux in the eddy correlation technique, is therefore defined across time, and the removal of trends from the data filters out low frequency oscillations that either represent organized large scale cycles within the selected time segment or span a time frame larger than that being studied, in which case they could represent 'mesoscale' or 'mesocycle' flux. By contrast, we define the instantaneous flux contributions within the 20 min time segment as 'local' flux events.

The accurate definition of the mean is an important aspect of the eddy correlation technique, and varying approaches may be found in the literature (Mahrt and Ek, 1993a; Caramori et al., 1994; Mitic et al., 1995 and 1997; Ogunjemiyo et al., 1997). Flux estimates are calculated by the covariance between the deviations of the vertical wind (w') and scalar admixtures (c') from their means. Implicit in this definition of a physically meaningful mean is the removal of any trends that might be present in the time series, as well as the separation of any large scale temporal cycles from the local instantaneous

flux events which are directly tied to the underlying surface and the time segment under study.

The local flux estimates were calculated using the fluctuations from the local means derived from linear detrending, in the form of a simple regression, and nonlinear detrending in the form of a truncated Fourier series. In cases where a nonlinear trends is present within the time series, the larger scale, mesocycle flux is derived from the low frequency oscillations filtered from the scalar concentration and the vertical wind field. The procedure is based on the decomposition of the flux into large scale time averages, represented by the mesoscale means and running (local) means represented by the linear or nonlinear series fitted to the data. Instantaneous fluctuations (w' and c') are defined against the local means, which may be non-stationary due to mesocycle 'events' (c^* and w^*). Considering this Reynolds type expansion into means and fluctuations, and the fact that $\langle c' \rangle$ and $\langle c^* \rangle$ (or $\langle w' \rangle$ and $\langle w^* \rangle$) vanish by definition, the time-averaged vertical flux F_T , over time T , at height h , is then given by

$$\begin{aligned} F_T &= \frac{1}{T} \int_T w(h, t) c(h, t) dt \\ &= \langle w \rangle \langle c \rangle + \langle c^* w^* \rangle + \langle c' w' \rangle \end{aligned} \tag{1}$$

In the case of $\langle w \rangle = 0$, which is a reasonable assumption for large, flat terrain such as the San Joaquin Valley, this expression is reduced to $F_T = \langle c^* w^* \rangle + \langle c' w' \rangle$, which is the sum of the mesocycle flux and the local flux respectively.

Using quadrant analysis, the modes of flux transport are defined for each flux event (Antonia, 1981; Grant et al., 1986). Each instantaneous contribution to the flux ($w'c'$) may be characterised according to the four modes of the eddy covariant transport as 'excess up' ($w^{(+)} c^{(+)}$), 'excess down' ($w^{(-)} c^{(+)}$), 'deficit up' ($w^{(+)} c^{(-)}$) and 'deficit down' ($w^{(-)} c^{(-)}$). Positive and negative fluctuations of the wind indicate updraft and downdraft, respectively. A correlation between the vertical fluctuation and the scalar fluctuation causes an average of the product to be non-zero, resulting in a contribution to the flux. This paper focuses on the gradient modes, which describe the dominant direction of flux, such as an upward transport of an excess of heat and moisture and a deficit of CO_2 and O_3 during daytime conditions. For night time conditions, upward gradient transport of heat and CO_2 is effected by an excess of CO_2 and deficit of heat. Downward gradient transport to the surface is characterised by an excess of CO_2 and O_3 and a deficit of heat and moisture during the day. The overall night time situation cannot be generalized for moisture and O_3 , and must be determined from the empirical data.

The separation of local flux from larger scale motions was followed by structural and coincident analyses to define the scales of coherent structures, their composition in terms of the fluxes they are simultaneously transporting and the degree of associations that exist between the various flux variables (Mitic et al., 1997). The horizontal extent of the structures is based on the Taylor frozen hypothesis (Taylor, 1938), assuming that the timescale for an eddy to evolve is longer than the time it takes to be advected past the sensor (Powell and Elderkin, 1974). The coherent structures are identified by a series of consecutive flux events within the same mode of transport, and the physical extent of

structures is given by the product of the duration of flux events within a certain transport mode and the corresponding wind speed. The minimum structure size is set at twice the size at which the instruments can resolve eddies, with the corresponding time scale determined by the minimum mean wind speed during the given 20 min periods, which defines the minimum time scale at which significant coherent contribution to flux could be resolved. Time scales (structures sizes) below this minimum are then disregarded as incoherent noise.

Coherent structures are initially defined for the individual flux parameters during the process of structural analysis. The flux variables, however, are not transported exclusively of each other, so that a coincident analysis is applied to resolve the distribution, size and composition of structures. The procedure combines coherent structures (defined for the individual flux variables) which overlap in their location along the time series, and therefore in spatial extent, and in the process identifies their composition in terms of water vapour, CO₂, heat and ozone, and their resultant sizes. The composition of these reconstituted structures are then used to define the degree of association among the fluxes. The absence of a particular flux from the composition of a structure indicates that for the duration of that structure, there was no consistent coherent contribution of that flux, i.e. in the sense that the minimum requirement for significant flux contribution was not met.

The association between fluxes, termed FA, is defined as a ratio (or percentage) of the number of structures with a particular composition, to the total number of structures defined for the 20 minute time series. Flux association for the four variables examined

may be defined for 15 categories based on the mutually exclusive combinations of CO₂, H₂O, heat and O₃. These combinations represent the presence of sustained coherent flux contribution within the structure. The absence of a particular flux from the composition of a structures does not indicate the total absence of that flux within that structure, but the absence of a minimum sustained coherent contribution for the duration of that structure. Using the above definition, a structure with a composition of H₂O and O₃ (HO), indicates that for the duration of the structure, only H₂O and O₃ had a sustained coherent flux contribution while the flux events of heat and CO₂ within that structure have been classified as incoherent noise. This technique is an improvement to the Jaccard coefficient used by Mitic et al. (1995), which defined flux associations (FA) based only on the coincidence of two scalars, and similar to that used by Mitic et al. (1997) with aircraft grid data sampled during CODE. The resulting flux associations eliminate ambiguity and are mutually exclusive for the various combination of scalars. The expression takes the form:

$$FA = \frac{C_{i,j,k,l}}{N-mp} \quad (2)$$

C_{i,j,k,l} is the number of coherent structures with the composition of scalars i, j, k, l (heat, H₂O, CO₂, O₃), or any combination of these ; N is the total number of structures (before reconstruction) for the overall time series; mp is the reduction in the number of structures as a result of overlap, so that N-mp is the total number of reconstructed structures.

During the process of defining the flux compositions of the structures, the mean flux of the individual components that make up that composition is also defined, a correlation analysis on associated fluxes within these classes is used to complement the flux association analysis, and structure sizes in relation to compositions is also examined.

3. RESULTS AND DISCUSSION

No consistent trends were observed in the data for both grape and cotton, for either night or day time series. For the majority of cases nonlinear detrending was most appropriate. Only in 5 of the 50 cases was linear detrending effective for the grape data and in 17 of 50 cases for the cotton data. In the case of nonlinear detrending, the filtered mesoscale flux accounted for 95% - 110% of the changes in the local flux estimates for the grape data and 84% - 111% for cotton, indicating successful isolation of the local fluxes from the larger mesocycles or mesoscale fluxes. The filtered mesoscale flux, however, was negligible and not considered in the subsequent analyses, which only examine the local instantaneous flux.

The mean flux densities for all cotton and grape data show the surface acting as a sink for CO_2 (C), and ozone (O) and a source of heat (T) and H_2O (H) during the day. During the night, it becomes a source of CO_2 , and a sink for heat, but remains a sink for ozone and a source of H_2O . This is seen in Figure 1, which also shows consistent dominance of latent heat flux over sensible heat flux during the day. The sensible heat fluxes from both grape and cotton are significantly lower around day of year (DOY) 211 to 215, a situation which is not reflected in the other variables. The observations shown

in Figure 1 allow for the definition of the gradient modes of transport of each flux during the day as well as - particularly - during the night.

3.1. Cotton Site Results

3.1.1. Flux Associations

The flux associations for all ten case studies are shown in Figure 2. The pattern of flux associations is similar for structures in both the gradient down and gradient up modes. Under **stable night time conditions**, structures associated with transporting only one flux component (CO_2 (C), H_2O (H), O_3 (O) or heat (T), exclusively) dominate, with flux association (FA) ranging from 35% to as high as 70%. This indicates the relative lack of mixing within the night-time collapsed boundary layer. The differential association of ozone with non- CO_2 transporting structures (no sustained presence of coherent CO_2 flux) during the night indicates the existence of a non-vegetated sink for ozone. The non-vegetated ozone sink is indicated by the relative prominence of structures transporting H_2O - O_3 -heat (HOT), which are also present during the day.

During **unstable day time conditions**, structures simultaneously transporting CO_2 - H_2O - O_3 -heat (CHOT) dominate, with FA between 26% and 57%, associated with the dominant vegetated sink. This indicates not only a higher degree of mixing, compared to the night-time cases, as would be expected, but presumably reflects also the co-located vegetated daytime source-sink for these variables. The association among structures transporting H_2O , O_3 and heat has the consistently second highest flux association. On DOY 213, however, structures transporting only CO_2 , H_2O and ozone figure more

prominently at 19%. This corresponds to the low sensible heat flux during this time (Figure 1) and is a direct result of the irrigation of the field. The association between the flux components of structures simultaneously transporting CHOT and HOT, indicating vegetated and non-vegetated source/sinks, respectively, was further documented by correlation analysis, as shown in Figures 3 and 4. For the CHOT structures, there is a consistent high correlation between H_2O and ozone, ranging from 0.68 to 0.91. The correlation between CO_2 and ozone is more variable (0.4 to 0.81) and reflects the correlation pattern between CO_2 and H_2O which is moderately high ranging from 0.5 to 0.8. There is also a consistent moderate to high correlation between heat and ozone within these structures (0.5 to 0.77). The correlation plots for the combined CHOT structures from all five days show a positive relationship among all the flux components. The corresponding correlation coefficients are also shown on the graphs in Figure 3 with the highest overall correlation between H_2O and ozone at 0.725. The mean structure flux intensities for the components of the CHOT structures may also be seen in Figure 4, with approximate maximum values of $-6.5 \text{ mg m}^{-2} \text{ s}^{-1}$ for CO_2 , $-4.5 \mu\text{g m}^{-2} \text{ s}^{-1}$ for ozone (where the negative sign indicates the surface as a sink), 2750 W m^{-2} for water vapour, and 750 W m^{-2} for heat. For structures transporting H_2O , O_3 and heat exclusively (HOT structures), the relationship between H_2O and ozone is even more pronounced with a correlation coefficient greater than 0.8 in all cases. The relationship between ozone and heat is more variable with a correlation coefficient ranging from 0.22 to 0.93, but in all cases less than that of H_2O and ozone. The relationship for the individual DOY is also reflected in the correlation coefficient for the combined cases shown in Figure 4, where the highest

correlation is between H_2O and ozone at 0.7. In general the correlation for all three fluxes is greater than 0.5. The above results suggest that in the well mixed daytime conditions over the cotton site, moisture and heat flux exert control over ozone flux with H_2O flux dominating in all cases.

3.1.2. Driving Forces

The presence/absence of heat and H_2O in the structure composition is directly related to the buoyancy flux which incorporates terms corresponding to both the heat flux and the water vapour flux. The buoyancy flux ($w'\theta'_v$), i.e. the virtual temperature flux associated with the moisture content of the air, was not explicitly calculated, but in the absence of liquid water in the air it can be approximated by

$$\overline{w'\theta'_v} \approx (\overline{w'\theta'}) [1 + 0.61\overline{r}] + 0.61\overline{\theta} (\overline{w'I'}) \quad (3)$$

where r is the water vapour mixing ratio (Stull, 1988). When $w'\theta'$ is negligible, the water vapour-related density effects dominate in buoyancy but even in the presence of significant heat flux the latter contribute significantly to buoyancy, as shown by the ratios of virtual density flux to sensible heat flux which were of the order of unity. In our analysis we differentiate between structures that have sensible heat and virtual temperature buoyancy effects from those that do not contain sensible heat flux, with a further category defined by the absence of buoyancy, presumably associated with shear forces. This partitioning of the driving forces operating at the cotton site during daytime conditions is shown in Figure 5. Heat is a contributing driving force in so far as 50% to 79% of the

structures have coherent heat flux in their composition. This is in contrast to the distribution of driving forces reported by Mitic et al. (1997) for aircraft grid flights (for CODE) at 30 m above the surface, where non-thermal forces played a more significant role. This may be an indication of the proportional changes in the surface-atmosphere dynamics with increasing height and spatial representation.

3.1.3. *Structure sizes and mean fluxes*

Structure size refers to the one dimensional horizontal extent (diameter) of the structure as defined in section 2. During stable night-time conditions the majority of the structures are less than 10 m in diameter. During the day, structure sizes extend up to 40 m. For these cases of unstable thermal conditions, the sizes of the structures simultaneously transporting CO_2 - H_2O - O_3 -heat (CHOT) and those transporting exclusively H_2O - O_3 -heat (HOT) are compared with the mean fluxes of the structure components. The CHOT structure sizes range from 3 m to 40 m, with the majority of structures less than 20 m. This corresponds to timescales of 1.5 to 26.6 s, with means ranging from 4.7 to 8 s. Figure 6 shows a scatter distribution of size and structure component mean fluxes for CHOT and HOT structures. The sizes for HOT structures range from 2 m to 32 m, with the majority of the structures sizes below 10 m. There is no clearly defined relationship between structure size and mean structure fluxes.

3.2. Grape Site Results

3.2.1 Flux Associations

The results from the FA analysis on the grape data are shown in Figure 7. The distribution of FA during **nighttime stable conditions** is very different from that of cotton. Here single component fluxes do not dominate, and ozone transport appears predominantly in association with that of CO₂. This suggests that a nonvegetated sink for ozone is not present. The consistently dominant structure compositions are CHOT with FA ranging from 16% to 29% and CHT with FA between 14% and 30%. This may reflect the much greater level of mixing during night-time stable conditions over grape, linked to the rougher canopy, as well as the greater measurement height over grape (almost twice that of cotton), and differences in the level of metabolic activity during the night. The FA during the **daytime unstable conditions** is similar to that of cotton with the majority of structures transporting CO₂, H₂O, ozone and heat (CHOT) simultaneously, and FA between 25% and 48%. Structures with fluxes of CO₂, H₂O and ozone (CHO) are also prominent during 2 sample periods with FA of 21% and 25%.

The indication of only one dominant ozone sink for grape, i.e. the one associated with vegetation, represents a significant difference between the FA for grape and cotton. The non-vegetated ozone sink at the cotton site may be the result of deposition to the soil and photochemical reactions with NO, as suggested by Massman et al., (1995) from examining ozone flux divergence between tower and aircraft flux.

The correlations within the dominant CHOT structures for unstable daytime conditions (Figure 8) are similar to those for cotton. There is a consistently high

correlation between CO₂ and ozone (0.57 to 0.97), H₂O and ozone (0.64 to 0.96), and CO₂ and H₂O (0.67 to 0.96). The CO₂-ozone relationship, however, does not indicate a dependence on the correlation between CO₂ and H₂O as appear to be the case over the cotton canopy. This difference may be due to the presence of only one vegetation based ozone sink for the grape site. The correlation for the combined CHOT structures for all five days are all very high with CO₂ and ozone at 0.88, H₂O and ozone at 0.86 and CO₂ and H₂O at 0.91. The correlation between heat and ozone, by contrast, is much lower at 0.49. The scatter plot in Figure 8 shows that there is a positive relationship among all four fluxes within the CHOT structures. The mean flux intensities for the components of the CHOT structures may also be seen from Figure 8, indicating approximate maximum values (excluding a few outliers) of -4.5 mg m⁻² s⁻¹ for CO₂, -3.5 µg m⁻² s⁻¹ for ozone, 3750 W m⁻² for water vapour and 450 W m⁻² for heat flux. Comparing the mean structure flux between grape and cotton, CHOT structures for cotton have a higher CO₂ flux, as may be expected given that the cotton crop was actively growing and accumulating biomass, as well as higher ozone and heat flux and lower H₂O flux. It should be considered that the partitioning of the energy fluxes depends on the dynamics of the rotating irrigation scheme. The findings on ozone flux correlate well with those of Massman et al. (1994, 1995), who found ozone flux to be higher at the cotton site than at the grape site. As suggested by Guo et al. (1995), the higher degree of wetness indicated by the higher H₂O flux and lower heat flux at the grape site would reduce the production of NO, accounting for the lower ozone flux as well as the absence of a dominant non-vegetated ozone sink.

3.2.2. *Driving Forces*

The breakdown of the driving forces during unstable conditions, shown in Figure 9, indicates that although heat remains a principal driving force for the surface fluxes (>50%), water vapour density gradients plays a more prominent role. This is especially true for days with significantly lower heat flux (211 and 212). The differences in the mix of driving forces, compared to that of cotton, may be partly attributed to the higher observation level over grape, as well as to the higher water vapour flux density within the dominant structures at that site. These results fall in between those for the cotton site at 5 m and those from aircraft data at 30 m (Mitic et al. 1997), giving a strong indication of the way in which the influence of the surface changes with height (Caramori et al., 1994), as well as of possible changes with the increased flux footprint (Schuepp et al., 1992).

3.2.3. *Structure sizes and mean fluxes*

The sizes for the dominant daytime CHOT structures (Figure 10) are larger than those over cotton, with a fairly even distribution between 1 m and 30 m corresponding to timescales of 1.7 to 27.6 s, with means ranging between 5.1 and 10 s. Similar to the distribution of driving forces, the structure sizes fall between those from the cotton site and those reported by Mitic et al., (1997) for aircraft data at 30 m. This may be an indication of the increased mixing and subsequent coalescing of structures with increasing height (Caramori et. al., 1994). Similar to the cotton canopy, there are no trends in the mean flux of the structure components and structure sizes.

4. CONCLUSION

The association of ozone to CO₂ and H₂O is not affected by the variations in the heat flux over the five sample days. During unstable conditions, structures transporting CO₂, H₂O, ozone and heat dominate for both the grape and cotton canopy. During stable conditions the flux association differs between cotton and grape, with the cotton canopy having more dominant single component structures. The results for the stable conditions, however, must be interpreted with caution in light of the very small magnitude for the fluxes and the difficulties associated with sampling under nighttime stable conditions.

The separation of ozone deposition into vegetative and non-vegetative sinks may be inferred from the proportion of structures transporting ozone in the presence and absence of CO₂. For the cotton site, a vegetated ozone sink associated with CHOT structures and a non-vegetated sink associated with HOT structures were observed. The grape site demonstrated only a vegetated sink for ozone associated to the dominant CHOT structures. These results may be compared with those of Mitic et al., (1997) for CODE aircraft data, where the dominant FA was CO₂, H₂O and ozone with no significant difference between the correlation of CO₂ and Ozone, and H₂O and ozone. The aircraft data, however, were obtained at a height of 30 m above a 15 x 15 km grid with varying crop and surface conditions. The differences may be reconciled to some extent by the smaller structure sizes and lower measurement height for the tower data, where structures are more tightly coupled to the surface, but where thermal forcing plays a more dominant role.

The structure sizes and corresponding timescales indicate that on average the dominant structures at the grape site are slightly larger than those at the cotton site but considerably smaller than those reported by Mitic et al., (1997) for aircraft data from CODE. These time scales and structures sizes fall within the lower end of the expected surface layer eddy scales and have potential for use as eddy scale limitation within simulation models.

Acknowledgement

The authors extend their thanks to the members of the Air Quality Research Division of Atmospheric Environment Service ,Canada , in particular, to G. den Hartog, R.E. Mickle, H.H. Neumann, J. Arnold, J. Deary and A. Beavan, for the use of the grape data. Our thanks also to Tony Delany, Steve Semmer, Tom Horst, Steve Oncley and Charlie Martin from the ASTER Facility at the National Centre for Atmospheric Research (NCAR) for the use of the cotton data. We especially express our appreciation to Jim Pederson and the California Air Research Board, and to the Natural Science and Engineering Research Council of Canada for funding this study.

References

Baldocchi, D.D., 1994: A comparison study of mass and energy exchange over a closed (wheat) and an open (corn) canopy. II: CO₂ exchange and water use efficiency, **Agri. Forest Meterol.**, **67**, 291-321.

Bonan, G.D., 1993: Importance of leaf area index and forest type when estimating photosynthesis in boreal forest, **Remote Sens. Environ.**, **43**, 303-314

Caramori, P., Schuepp, P.H., Desjardins, R.L., and MacPherson, J.I., 1994: Structural analysis of airborne flux measurements over a region, *J. Climate*, **7**, 627-640

Chapman, S.J., and M. Thurlow, 1996: The influence of climate on CO₂ and CH₄ emissions from organic soils, *Agri. and Forest Meteor.* **79**, 205-217

D'Arrigo, Rosanne, Jacoby, Gordon, C., and Inez Y. Fung, 1987: Boreal forest and atmosphere-biosphere exchange of carbon dioxide, *Nature*, **329**, 321-323

Eloranta, E.W., Forrest D.K., 1992. Volume imaging lidar observations of the convective structure surrounding the flight path of a flux-measuring aircraft, *J. Geophys. Res.*, **97**(D17): 18,383-18,498

Field C.B., Chapin III, F.S., Matson, P.A., and H.A. Mooney, 1992: Responses of terrestrial ecosystems to the changing atmosphere, *Annual Review of Ecology and Systematics*, **23**, 210-235

Goetz, Scott J., and Stephen D. Prince, 1996: Remote Sensing of net primary production in boreal forest stands, *Agri. Forest Meteor.*, **78**, 149-179

Guo, Y., Desjardins, R.L., MacPherson, J.I., and Schuepp, P.H., 1995a: The correspondence of aircraft-measured fluxes of sensible heat, latent heat, CO₂, and ozone to the surface characteristics in the San Joaquin valley of California, *Atmos. Environ.*, **29**, (21), 3159-3168

Guo, Y., Desjardins, R.L., MacPherson, J.I., and Schuepp, P.H., 1995b: A simple scheme for partitioning aircraft-measured ozone fluxes into surface uptake and chemical transformation, *Atmos. Environ.*, **29**, (21), 3199-3207

Hall, Forrest G., Shimabukuro, Yosio E., and Karl F. Huemmrich, 1995: Remote sensing of forest biophysical structure using mixture decomposition and geometric reflectance model, *Ecological Applications*, **5**, (4), 993-1013

Hanan, N.P., Prince, S.D. and A. Begue, 1995: Estimation of absorbed photosynthetically active radiation and vegetation net production efficiency using satellite data, *Agri. Forest Meteor.*, **76**, 259-276

Harris, R.C., and S.E. Frolking, 1992: The sensitivity of methane emissions from northern freshwater wetlands to global warming. In: P. Firth and S. Fisher (eds.) *Global Climate Change and Freshwater Ecosystems*, Springer Verlag, New York, pp. 48-67

Hollinger, D.Y., Kelliher, FM., Byers, J.N., Hunt, J.E., McSeveny, T.M and P.L. Weir, 1994: Carbon dioxide exchange between an undisturbed old-growth temperate forest and the atmosphere, **Ecology**, **75**, 134-150

Klaassen, Wim, and Martin Claussen, 1995: Landscape variability and surface flux parameterization in climate models, **Agri. and Forest Meteor.**, **73**, 181-188.

Koster, R.D., and M.J. Suarez, 1992: Modelling the land surface boundary in climate models as a composite of independent vegetation stands, **J. Geophys. Res.**, **97**, (D3), 2697-2715

Lee, Xuhui, Black, Andrew T., den Hartog, Gerry, Neumann, Harold H., Nesic, Zoran, and Janusz Olejnik, 1996: Carbon dioxide exchange and nocturnal processes over a mixed deciduous forest, **Agri. Forest Meteor.**, **81**, 13-29

Mack, A.R., Dejardins, R.L., MacPherson, J.I., and P.H. Schuepp, 1990: Relative Photosynthetic Activity of Agricultural Lands from Airborne Carbon Dioxide and Satellite Data, **Int. J. Remote Sens.**, **11**, (2), 237-251

Mahrt, H. and EK, M., 1993a: Mesoscale (subgrid) variability of turbulent fluxes in HARPEX and CODE, **Proc. Conf. on Hydroclimatology**, Americ. Meteorol. Soc., Anaheim, Calif., Jan. 17-22, 1993, 130-131.

Mahrt, H. and EK, M., 1993b: Spatial variability of Turbulent fluxes and roughness lengths in HARPEX-MOBILHY, **Boundary Layer Meteorology**, **65**, 381-400

Massman, W.J., Pederson, J., Delany, A., den Hartog, G., Neumann, H.H., Grantz, D. and Pearson Jr., R., 1993: A Comparison of independent determinations of the canopy conductance for carbon dioxide, water vapour and ozone exchange at selected sites in the San Joaquin valley of California, **Proc. Conf. on Hydroclimatology**, Americ. Meteorol. Soc., Anaheim, Calif., Jan. 17-22, 1993, 112-117

Massman, W.J., Pederson, J., Delany, A., Grantz, D., den Hartog, G., Neumann, H.H., Oncley, S.P., Pearson Jr., R., and Shaw, R.H. 1994: An evaluation of the regional acid deposition model surface module for ozone uptake at three sites in the San Joaquin Valley of California, **J. Geophys Res.** **99** (D4), 8281-8294

Massman, W.J., MacPherson, J.I., Delany, A., den Hartog, G., Neumann, H.H., Oncley, S.P., Pearson Jr., R., Pederson, J., and Shaw, R.H. 1995: Surface conductance for ozone uptake derived from aircraft eddy correlation data, **Atmos. Environ.** **29**, **21**, 3181-3188

McGuire, A.D., Melillo, J.M., Joyce, L.A., Kicklighter, D.W., Grace, A.L., Moore, B. and C.J. Vorosmarty, 1991: Interactions between carbon and nitrogen dynamics in estimating net primary productivity for potential vegetation in North America, **Global Biogeochem. Cycles**, **6**, 101-124.

Melillo, Jerry M., McGuire, David A., Kicklighter, David W., Moore III, Berrien, Vorosmarty Charles J., and Annette L. Schloss, 1993: Global climate change and terrestrial net primary production, **Nature** **363**, 234-240

Mitic, C.M., Schuepp, P.H., Desjardins, R.L., and I.J. MacPherson, 1995: Spatial distribution and co-occurrence of surface-atmosphere energy and gas exchange processes over the CODE grid site, **Atmos. Environ.**, **29**, (21), 3169-3180

Mitic, Constance M., Schuepp, Peter H., Desjardins, Raymond L., and Ian J. MacPherson, 1997: Flux association in coherent structures transporting CO₂, H₂O, heat and ozone over the CODE grid site, **Agri. Forest Meteor.** (in press).

Mooney, H.A., Drake, B.G., Luxmoore, R.J., Oechel, W.C., and L.F. Pitelka, 1991: Predicting Ecosystem Responses to Elevated CO₂ Concentrations: What has been learned from laboratory experiments on plant physiology and field observations?, **Bioscience** **41**, (2), 96-104

Moore, C.E., Fitzjarrald, D.R., and J.A. Ritter, 1993: How well can regional fluxes be derived from smaller scale estimates? **J. Geophys. Res.**, **98**, 7177-7198

Ogunjemiyo, S.O., Schuepp, P.H., MacPherson, J.I., and Desjardins, R.L., 1997: Analysis of flux maps vs. Surface characteristics from Twin Otter grid flights in BOREAS 1994, **J. Geophys. Res.** (In Press)

Paw U, Kyaw Tha; Qiu, Jie; Su, Hong-Bing; Watanabe, Tomonori, and Yves Brunet, 1995: Surface renewal analysis: a new method to obtain scalar fluxes, **Agri. Forest Meteor.** **74**, 119-137

Pederson, J.R., Massman, W.J., Mahrt, L., Delany, A., Oncley, S., Den Hartog, G., Neumann, H.H., Mickle, R.E., Shaw, R.H., Paw U, K.T., Grantz, D.A., MacPherson, J.I., Desjardins, R., Schuepp, P.H., Pearson Jr, R., and Arcado, T.E., 1995: California Ozone Deposition Experiment: Methods, results and opportunities. **Atmos. Environ.**, **29**, (21), 3115-3132

Powell, D.C., and Elderkin, C.E., 1974: An investigation of the application of Taylor's hypothesis to atmosphere boundary layer turbulence, **J. Atmos. Sc.** **31**, 990-1002

Rochette, P., Desjardins, R.L., Patty, E. and R. Lessard, 1994: Measurement of crop net carbon dioxide exchange rate in soybean, **21st AFM Conference on Agricultural and Forest Meteorology**, pp 259-260, (preprint).

Ruirmy, Anne; Kergoat, Laurent; Field, Christopher and Bernard Saugier, 1996: The use of CO₂ flux measurements in models of the global terrestrial carbon budget, **Global Change Biology**, **2**, 287-296

Schuepp, P.H., Desjardins, R.L., MacPherson, J.I., Boisvert, J., and L.B. Austin, 1987: Airborne determination of regional water use efficiency and evapotranspiration: present capabilities and initial field tests. **Agric. Forest Meteor.**, **41**, 1-19

Schuepp, P.H., MacPherson, J.I., and R.L. Desjardins, 1992: Adjustment of footprint correction for airborne flux mapping over the FIFE site. **J. Geophys. Res.** **97**, (D17), 18455-18466

Stull, Roland B., 1988: **An Introduction to Boundary Layer Meteorology**, Kluwer Academic Press, Dordrecht, The Netherlands, 666 pgs.

Sud, Y.C., Shukla, J., and Y. Mintz, 1988: Influence of land surface roughness on atmospheric circulation and rainfall. A simulation with a general circulation model, **J. Appl. Meteor.**, **27**, 1036-1054

Taylor, G.I., 1938: The Spectrum of Turbulence, **Proc. R. Soc.**, A164, 476-490

Viau, Alain A., and Constance M. Mitic, 1992: Potential impacts of CO₂-induced climate change using the GISS, GFDL and CCC scenarios on corn yields in the Essex county region of Ontario, **Climatological Bulletin**, **26**, (2), 79-105

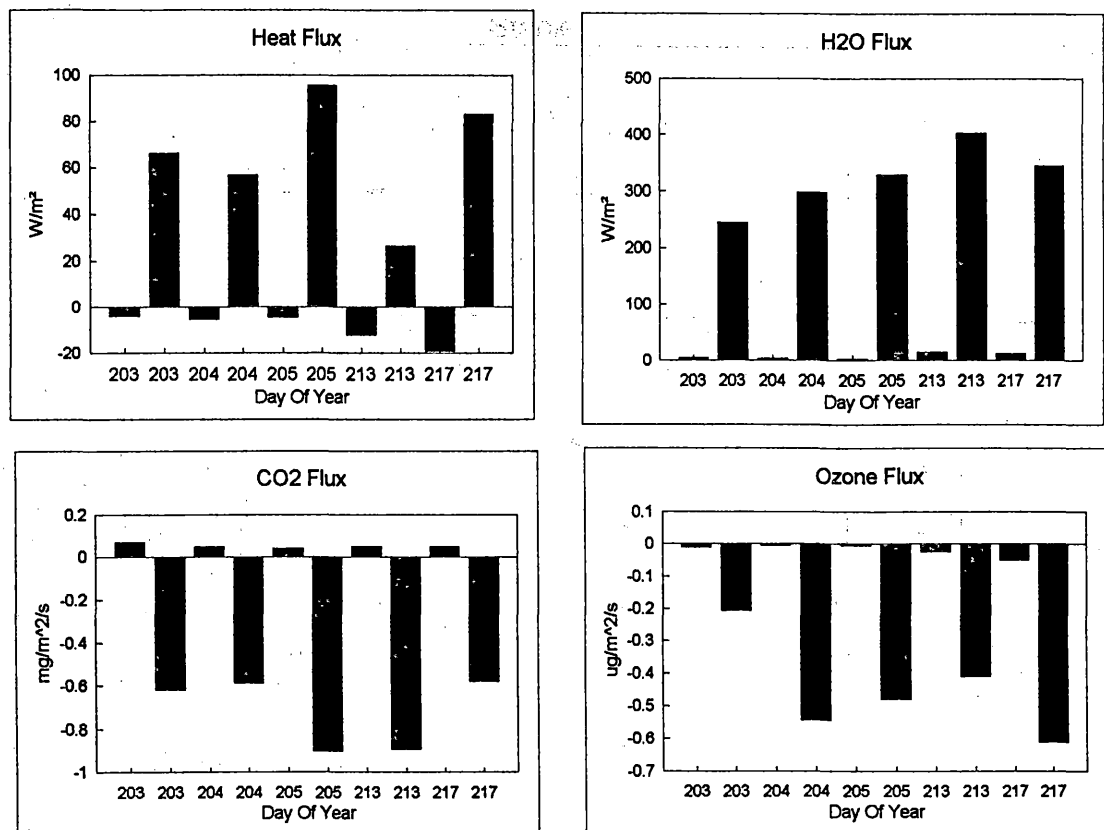
Wollenweber, Gabriel C., 1995: Influence of fine scale vegetation distribution on surface energy partition, **Agri. Forest Meteor.**, **77**, 225-240

Wyngaard, J.C., 1983: Lectures on the planetary boundary layer. In: D.K. Lilly and T. Gal-Chen (eds.) **Mesoscale Meteorology Theories, Observations and Models**. Reidel Publ., Dordrecht, pp. 603-650 and pp. 216-224

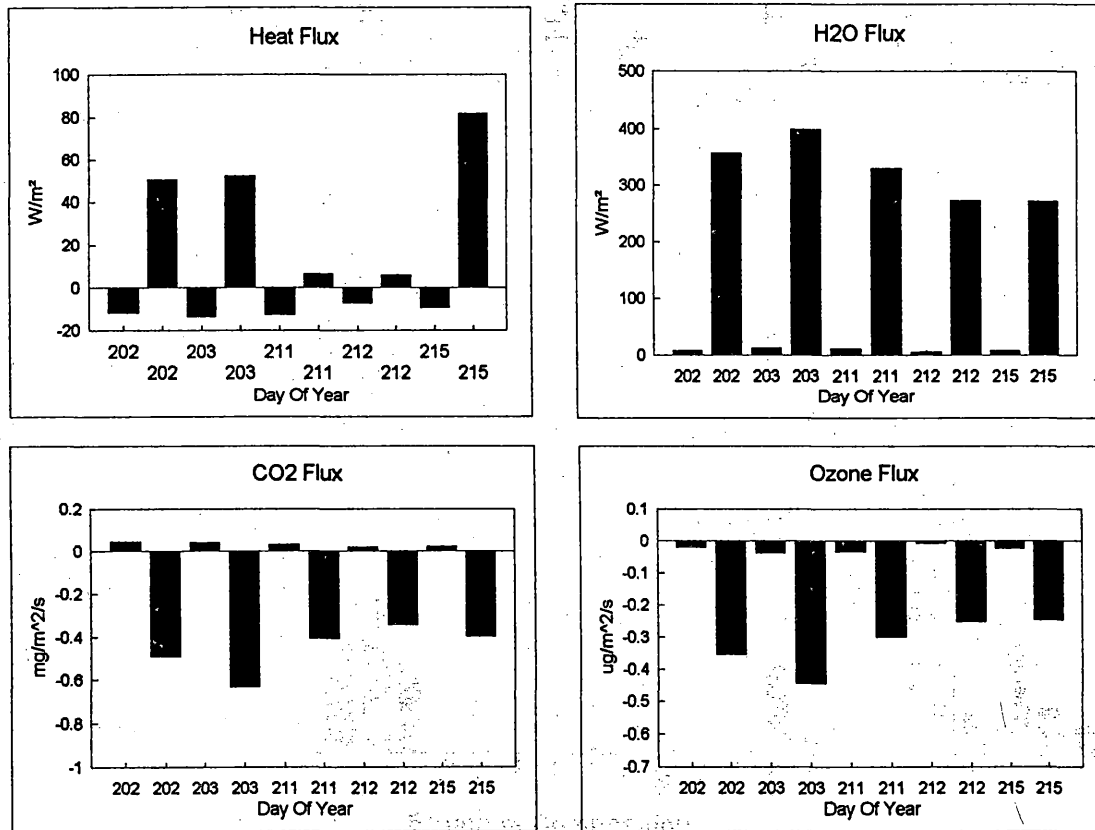
	Cotton		Grape	
	<i>night</i>	<i>day</i>	<i>night</i>	<i>day</i>
July 22			4:00 am	1:30 pm
July 23	1:00 am	12:00 pm	1:00 am	12:00 pm
July 24	4:00 am	1:30 pm		
July 25	4:00 am	12:30 pm		
July 30			1:00 am	12:00 pm
July 31			4:00 am	2:30 pm
August 01	3:30 am	1:00 pm		
August 03			12:30 am	1:00 pm
August 05	9:30 pm	3:30 pm		

Table 1. Selected dates and start time of the 20 minute segments used as case studies for the cotton and grape sites. Times are in pacific local time, and night refers to conditions of zero solar radiation.

Mean Fluxes for 20 minute time segments
Cotton site



Grape site



note: Bars in the order of night-day

Figure 1.

Flux Association at the Cotton Site

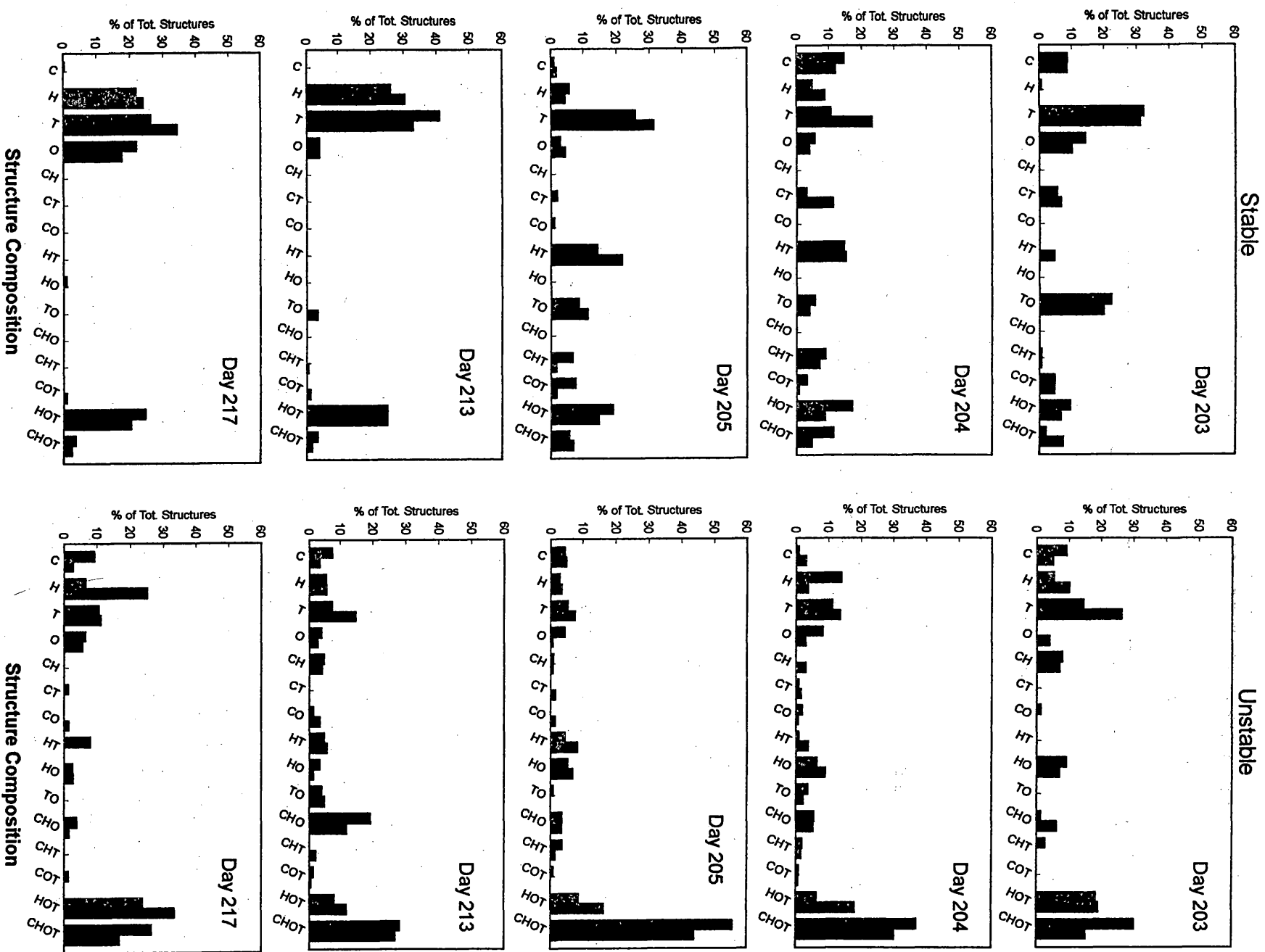


Figure 2.

Correlation Analysis within Dominant Gradient up Structures
Cotton site : Unstable conditions

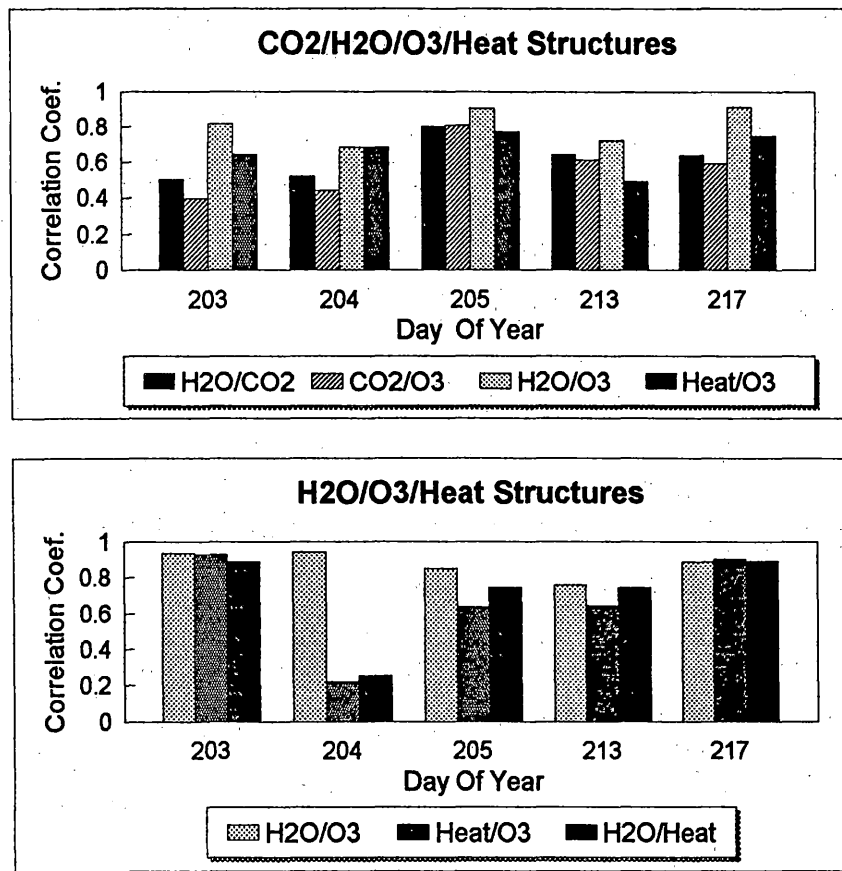
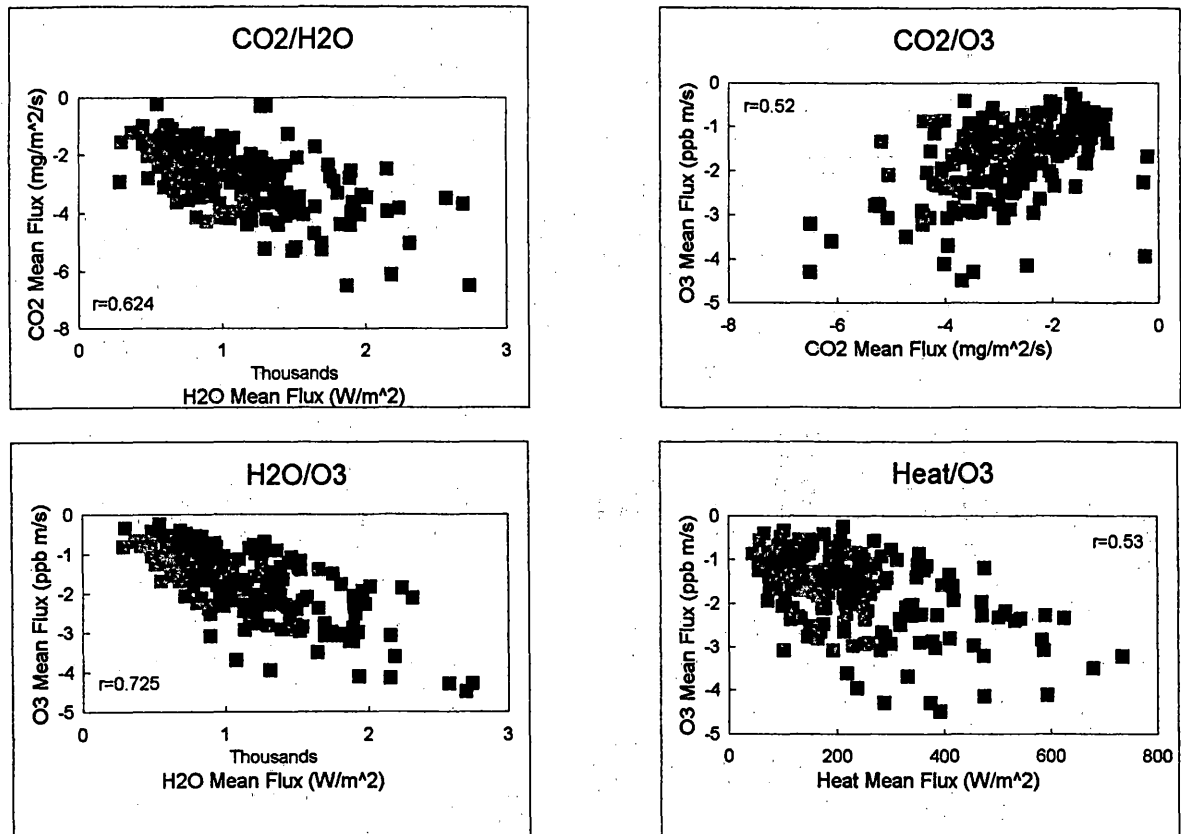


Figure 3.

Correlation Analysis : Cotton site : Unstable conditions
CHOT Structures



HOT Structures

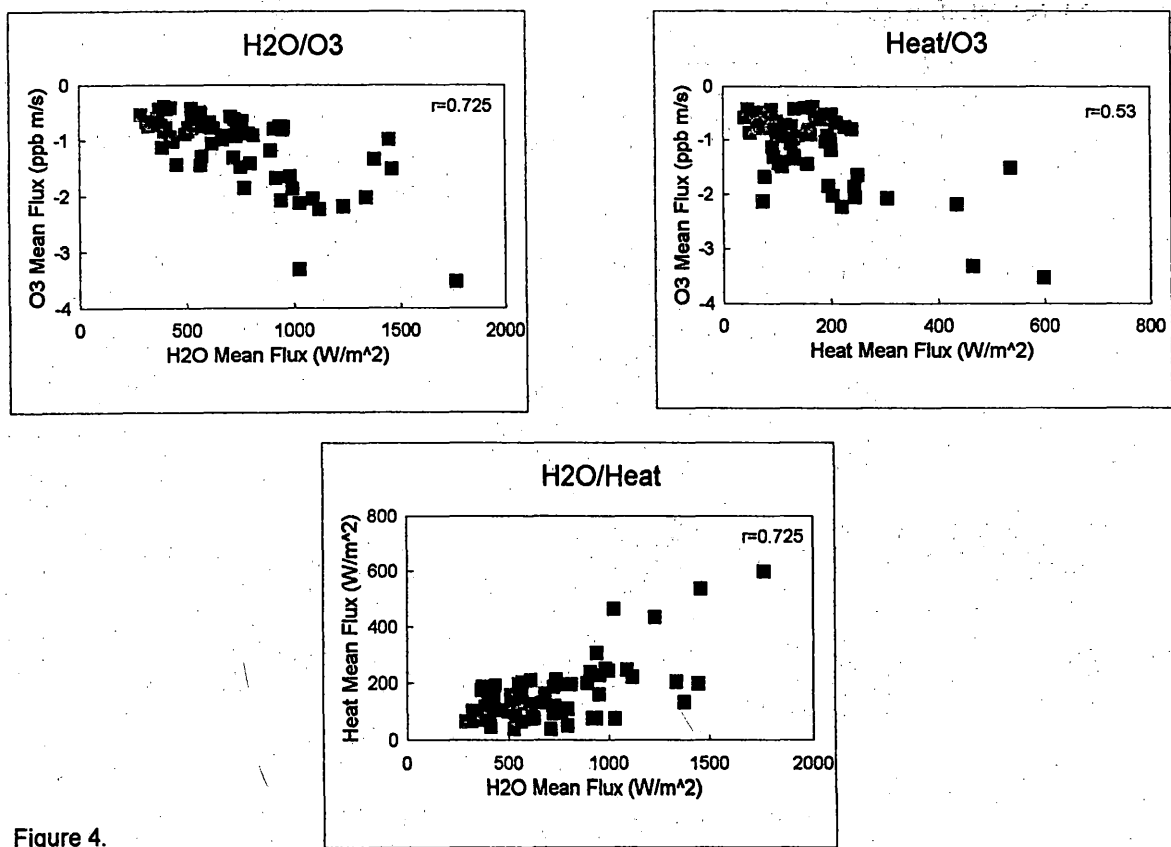


Figure 4.

Driving Forces during Unstable Condition Cotton Site

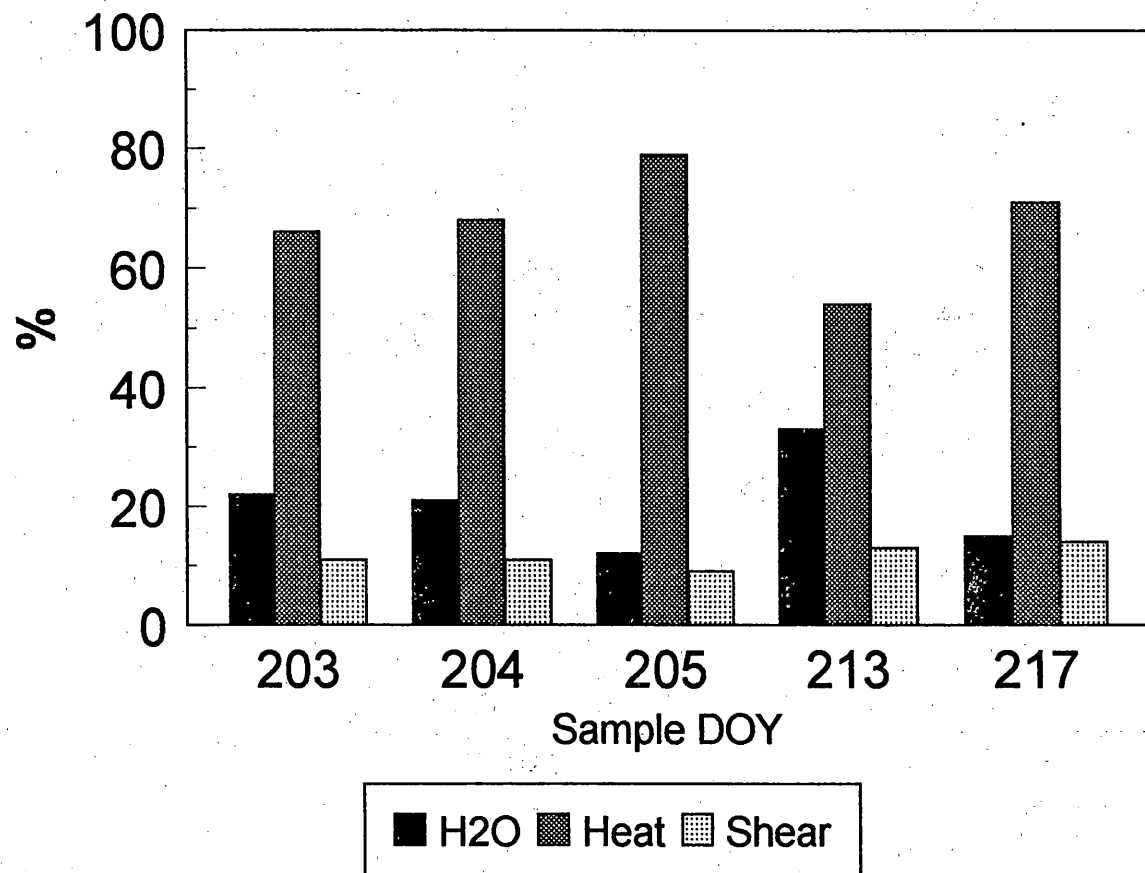
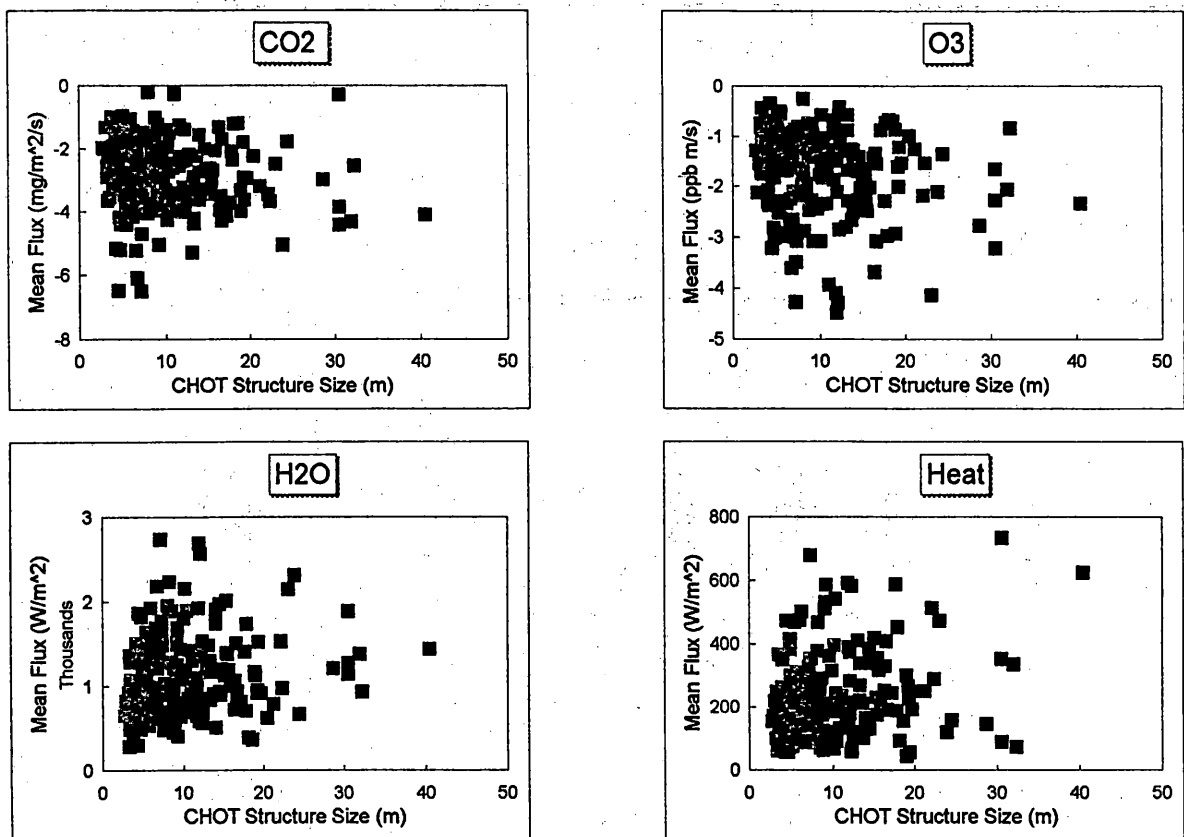


Figure 5.

Structures Size Distribution and Mean Fluxes: Cotton site : Unstable conditions
CHOT Structures



HOT Structures

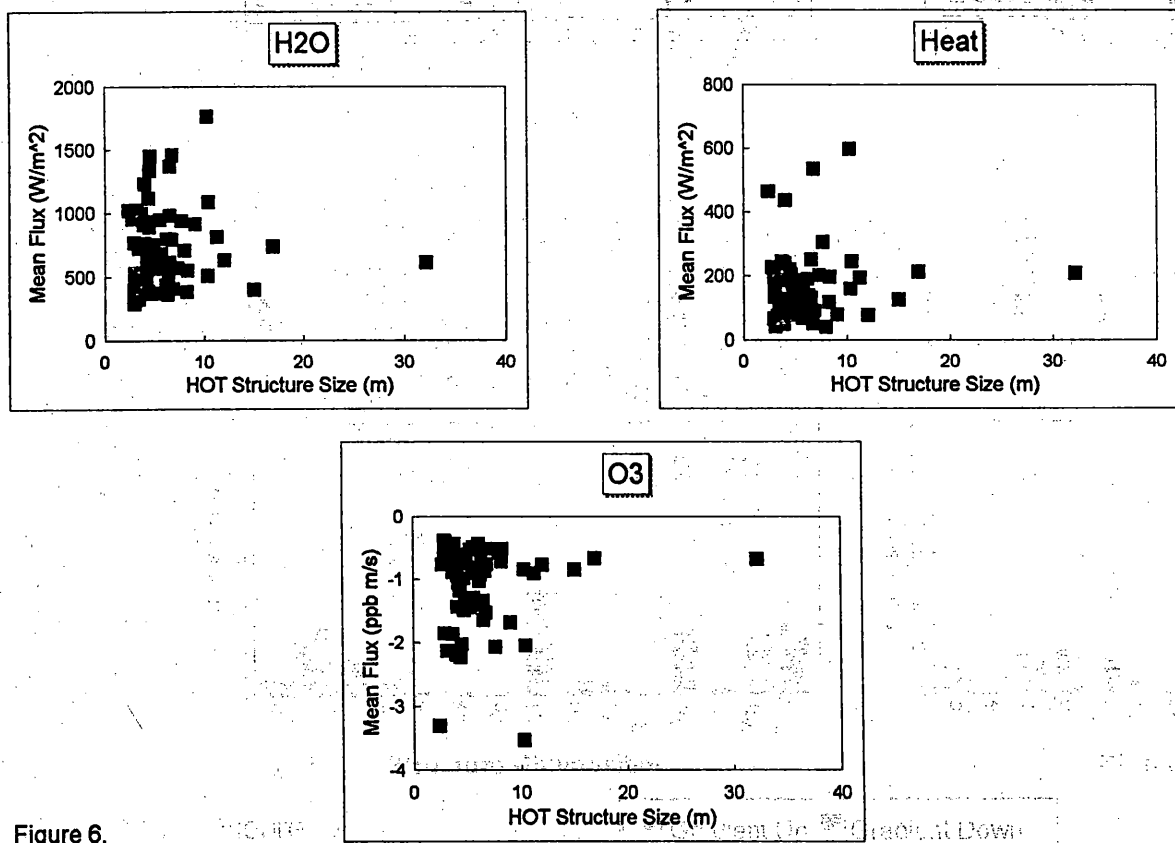


Figure 6.

Flux Association at the Grape Site

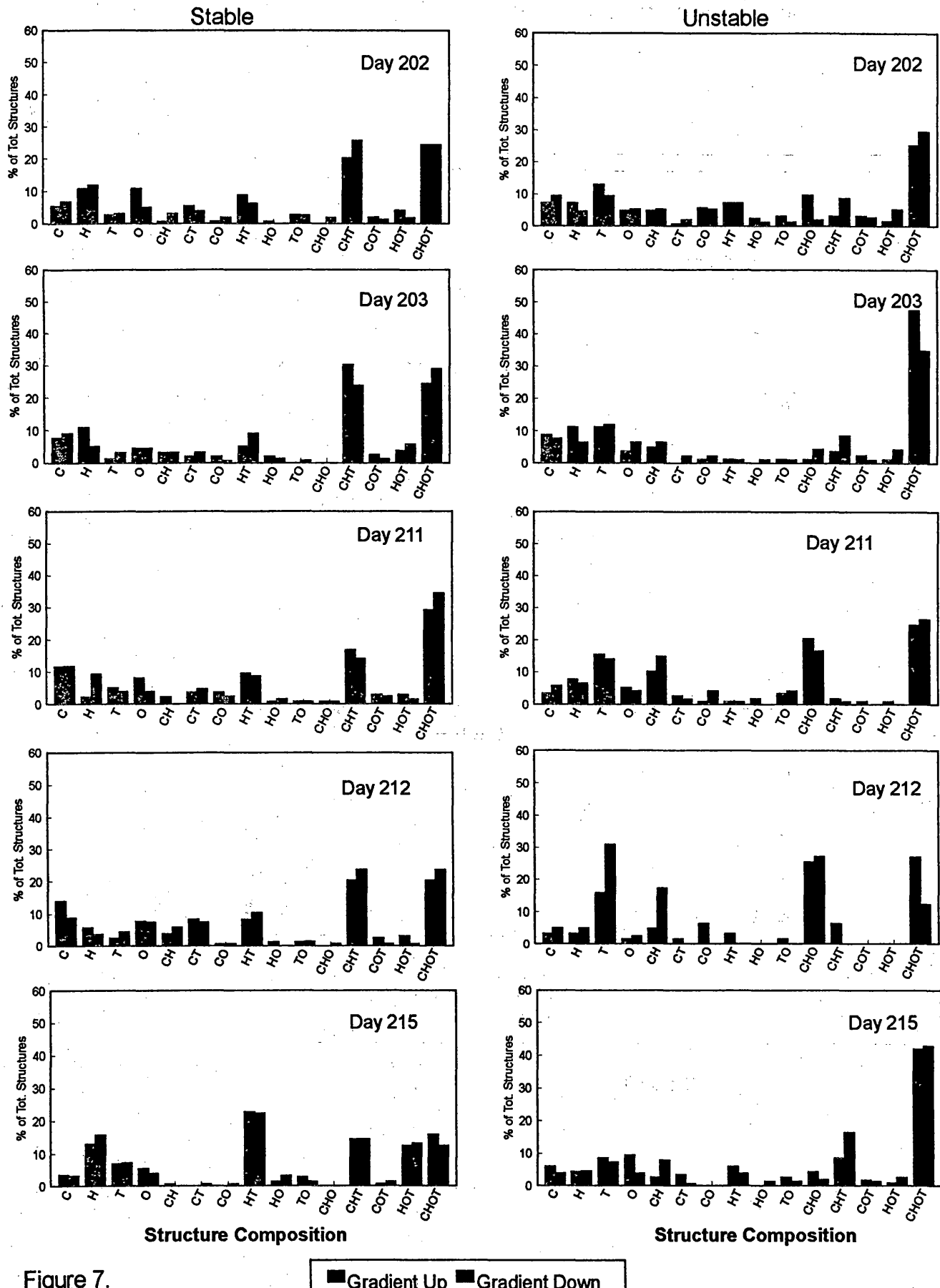


Figure 7.

Correlation Analysis within CO₂/H₂O/O₃/Heat structures
Grape site : Unstable conditions

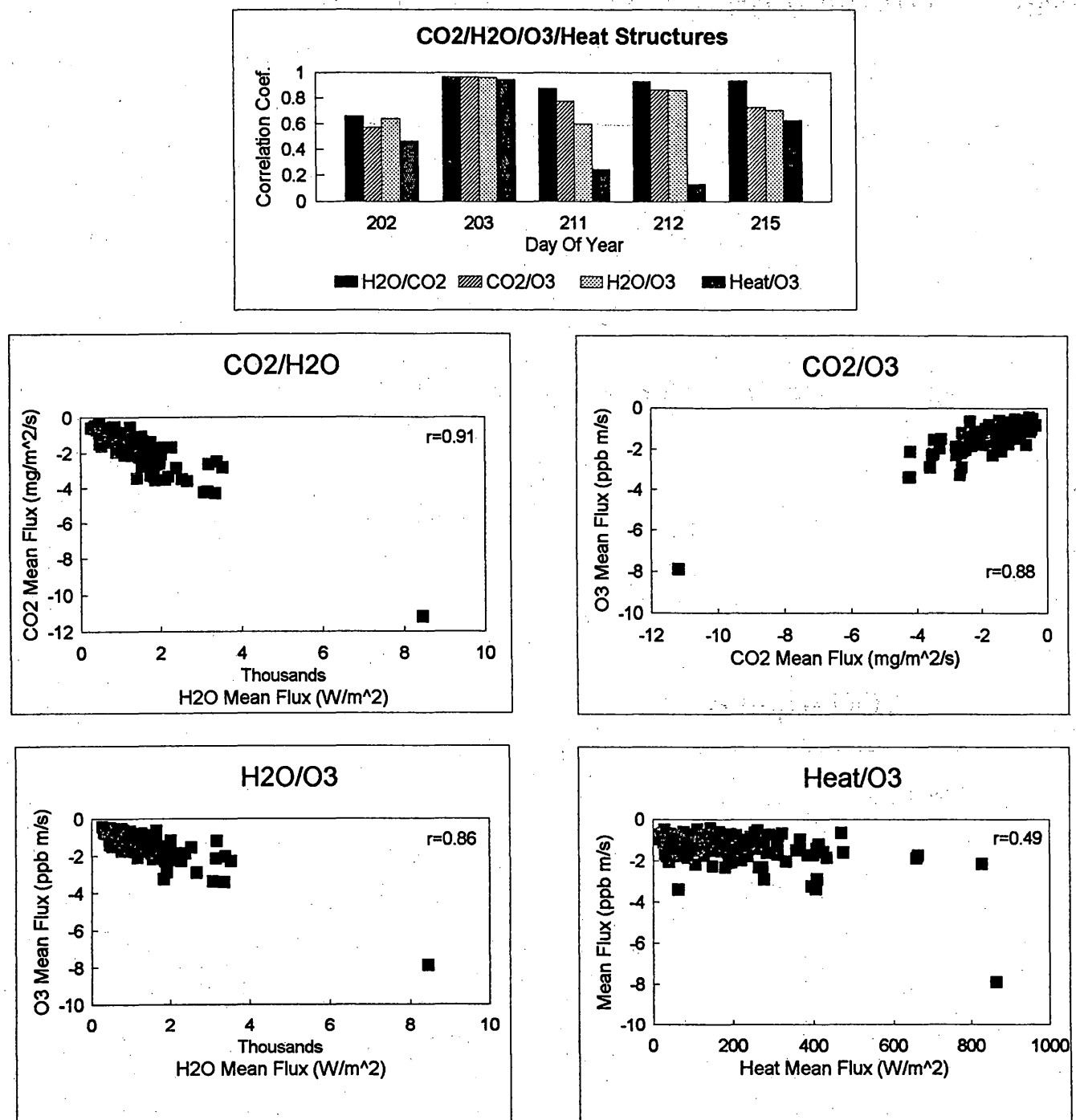


Figure 8.

Driving Forces during Unstable Condition Grape Site

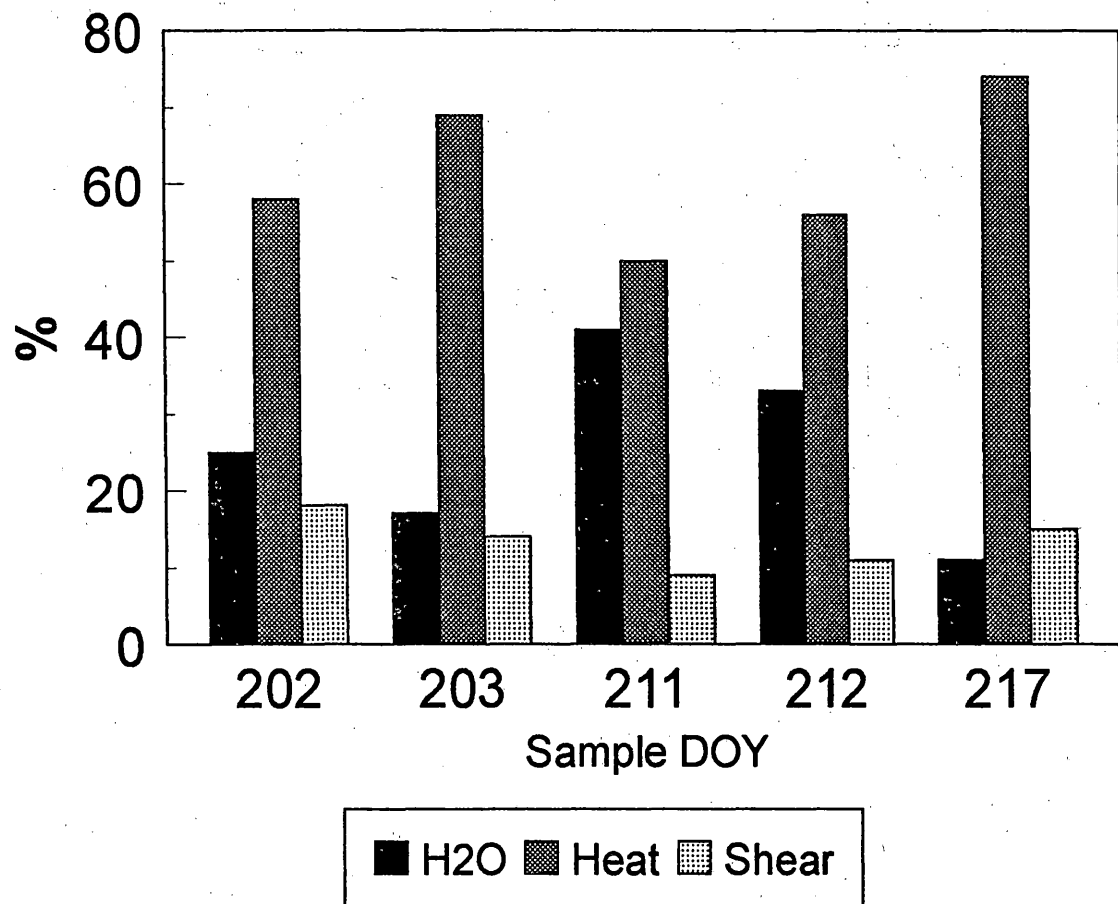


Figure 9.

Structures Size Distribution and Mean Fluxes: Grape site : Unstable conditions
CHOT Structures

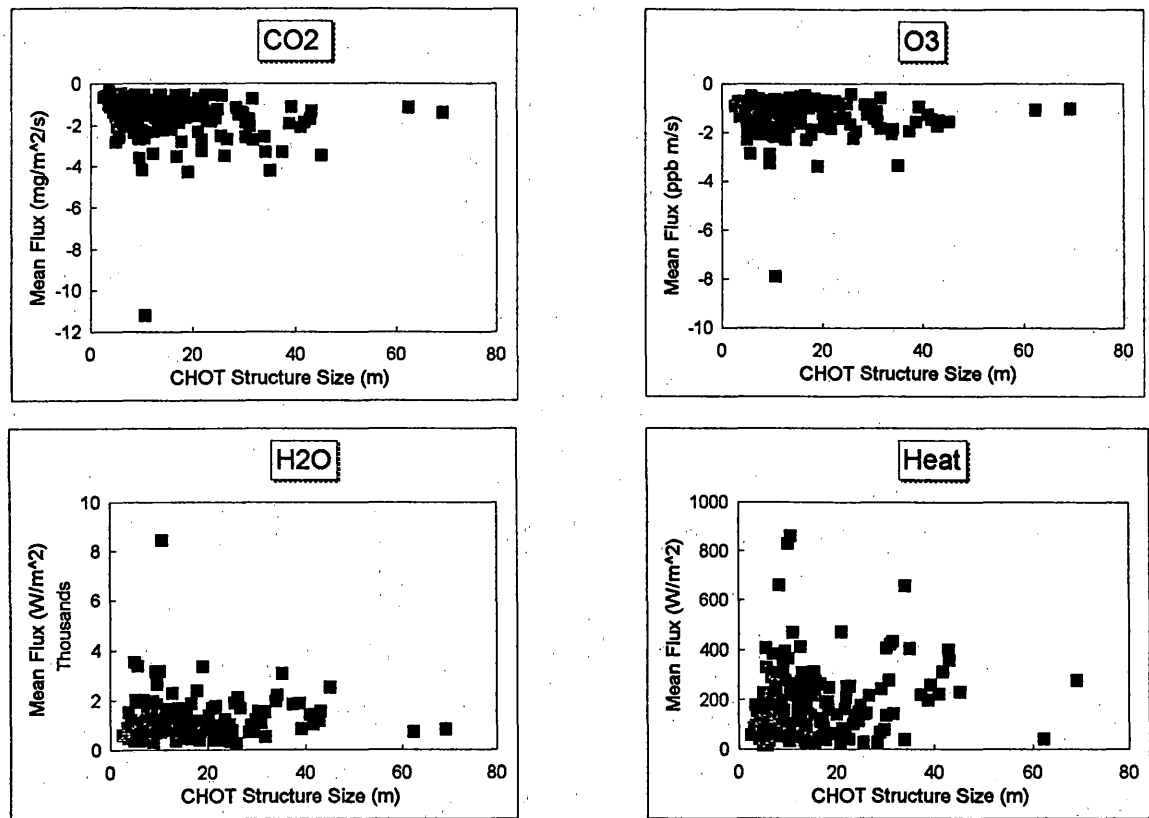


Figure 10.